Published in final edited form as:
Cancer Res. 2013 April 15; 73(8): 2493–2504. doi:10.1158/0008-5472.CAN-12-4241.

Chemotherapy acts as an adjuvant to convert the tumor microenvironment into a highly permissive state for vaccination-induced antitumor immunity

Tae Heung Kang[1], **Chih-Ping Mao**[1], **Sung Yong Lee**[1,5], **Alexander Chen**[1], **Ji-Hyun Lee**[6], **Tae Woo Kim**[7], **Ronald D. Alvarez**[8], **Richard B.S. Roden**[1,2,4], **Drew Pardoll**[1,4], **Chien-Fu Hung**[1,4], and **T-C Wu**[1,2,3,4]

[1]Department of Pathology, Johns Hopkins Medical Institutions, Baltimore, Maryland, USA

[2]Department of Obstetrics and Gynecology, Johns Hopkins Medical Institutions, Baltimore, Maryland, USA

[3]Department of Molecular Microbiology and Immunology, Johns Hopkins Medical Institutions, Baltimore, Maryland, USA

[4]Department of Oncology, Johns Hopkins Medical Institutions, Baltimore, Maryland, USA

[5]Department of Internal Medicine, Korea University Medical Center, Seoul, South Korea

[6]Department of Molecular Cell Biology and Samsung Biomedical Institute, Sungkyunkwan University School of Medicine, Suwon, Gyeonggi-do, South Korea

[7]Division of Infection and Immunology, Graduate School of Medicine, Korea University, Seoul, South Korea

[8]Department of Obstetrics and Gynecology, University of Alabama at Birmingham, USA

Abstract

Multiple classes of pharmacologic agents have the potential to induce the expression and release of pro-inflammatory factors from dying tumor cells. As a result, these cells can in theory elicit an immune response through various defined mechanisms to permanently eradicate disseminated cancer. However, the impact of chemotherapy on the tumor-specific immune response in the context of the tumor microenvironment is largely unknown. Within the tumor microenvironment, the immune response promoted by chemotherapy is antagonized by an immune-suppressive milieu, and the balance of these opposing forces dictates the clinical course of disease. Here we report that high antigen exposure within the tumor microenvironment following chemotherapy is sufficient to skew this balance in favor of a productive immune response. In elevating antigen exposure, chemotherapy can achieve long-term control of tumor progression without the need of an additional adjuvant. We found that chemotherapy initiated this phenomenon in the tumor microenvironment through an accumulation of dendritic cells, which stimulated CD8+ T cells and the type-I interferon pathway. From this conceptual base, we developed a simple approach to cancer therapy combining chemotherapy and vaccination that may be widely applicable.

Address correspondence to: Dr. T-C Wu, Professor, Department of Pathology, Johns Hopkins, Medical Institutions. CRB II Room 309, 1550 Orleans St., Baltimore, MD 21231. Phone: (410), 614-3899; Fax: (443) 287-4295; wutc@jhmi.edu.

Conflict of Interest:
Richard Roden has received grant support from Sanofi Pasteur and GlaxoSmithKline and has ownership interests in PaxVax and Papivax. Drew Pardoll has served as a consultant or on an advisory board for Bristol-Meyers Squibb, AmpImmune and ImmuneXcite, without compensation. All other authors declare they have no conflicts of interest.

Keywords

Chemotherapy; tumor microenvironment; cisplatin; vaccination

Introduction

It is now clear that multiple classes of pharmacologic agents for cancer therapy have the potential to elicit the release of pro-inflammatory substances from dying tumor cells (1, 2). These substances are able to induce the maturation of dendritic cells (DCs) and the subsequent activation of tumor-specific $CD8^+$ cytotoxic T lymphocytes (CTLs). Indeed, it has been shown that, when pre-treated with chemotherapy, tumor cells can evoke a robust adaptive immune response upon transfer into mice (1, 2). Furthermore, these mice efficiently reject secondary tumor challenge (1, 2). Several reports over recent years have revealed that the mechanisms underlying the inflammatory effects of chemotherapy are numerous and diverse, involving for example activation of the NLRP3 inflammasome (3), surface translocation of calreticulin (4), autophagy and ATP release (5), instigation of the endoplasmic reticulum stress response (6), caspase activation (7), or secretion of HMGB1 (8).

The immune response produced by tumor cells mixed with chemotherapy—together with our knowledge of the molecular mechanisms underlying this process—has fueled much of the enthusiasm for combining chemotherapy with immune-based therapy (9). The rationale for this dual approach is that chemotherapy—a mainstay intervention for cancer since the 1940s—has the potential to debulk the primary tumor mass, while immune-based therapy has the potential to eradicate disseminated disease and to prevent relapse. Thus, this dual approach represents a synergistic strategy that capitalizes on the strengths of each therapy while circumventing its major weaknesses. Furthermore, it is well established that chemotherapy can induce an inflammatory state in tumor cells (1, 2) and the effects of chemotherapy on the tumor microenvironment in the context of the host immune response are becoming better understood (10-13). While chemotherapy would in theory elicit the release of pro-inflammatory substances from cancer cells in such a microenvironment, the tumor milieu also contains a host of elements that dampen the anti-tumor immune response, such as suppressive cytokine networks, immune checkpoints, and regulatory subsets of cells (14). These elements are largely responsible for the failure of immune-based therapy in the clinic. Therefore, in order for a dual approach combining chemotherapy and immune-based therapy to be successful for cancer patients, chemotherapy must be able to overcome the obstacles to immune-based therapy posed by the tumor microenvironment. The purpose of the current study is thus to characterize the effects of chemotherapy on the immune response within the tumor microenvironment and to uncover the mechanisms responsible for these effects.

We found that chemotherapy converts the tumor into a site permissive for the activation of an adaptive immune response within the tumor. Notably, this immune response can be produced with a vaccination lacking adjuvant, which represents a marked advantage over other types of immune-based therapy. Also, we found that this immune response is driven by the accumulation of DCs in the tumor, followed by their maturation, migration to lymph nodes, and priming of tumor-specific $CD8^+$ CTLs in a type I-interferon-dependent manner. Our data further indicate that antigen density within the tumor is an important determinant of the outcome of immune surveillance following chemotherapy. With this concept, we create an effective, universally applicable strategy for cancer therapy based on systemic antigen delivery to the tumor.

Methods

Mice

6- to 8-week-old female C57BL/6 or BALB/c mice were obtained from the National Cancer Institute. TLR4 knockout mice were from the Jackson Laboratory, and IFNAR knockout mice were a kind gift from Dr. G. Cheng laboratory (University of California, Los Angeles, Los Angeles, CA). All animal procedures were performed under protocols approved by the Johns Hopkins Institutional Animal Care and Use Committee and in accordance with recommendations for the proper use and care of laboratory animals.

Cells

The TC-1 tumor model **was generated** by transformation of primary lung epithelial cells from C57BL/6 mice with active Ras together with HPV-16 E6 and E7 oncogenes and the production and maintenance of this cell line has been described previously (15). TC-1 cells were subjected to RapidMAP (Taconic Farms, Rensselaer, NY) testing, a panel of PCR tests for rodent viruses, most recently in May 2011 with negative results. CT26 colon carcinoma cells were obtained **from the ATCC cell bank**, which characterized the cell line for mycoplasma by the Hoescht stain, PCR and the standard culture test, all of which had negative results. Cells were cultured at 37°C with 5% CO_2 in RPMI-1640 medium supplemented with 10% fetal bovine serum, 2 mM L-glutamine, 1 mM sodium pyruvate, 2 mM non-essential amino acids, and 50 U/ml penicillin/streptomycin.

Tumor treatment experiments

TC-1 or CT26 tumor cells (10^5 per animal) were inoculated subcutaneously into C57BL/6 or BALB/c mice (10 per group), respectively. 5 days later, tumor-bearing mice were treated i.t. with 20 μg of E7 peptide (aa42-63) or AH1-A5 (SPSYAYHQF), or 50 μg of TA-CIN recombinant protein or isotonic saline control, in conjunction with intraperitoneal cisplatin (5 mg/kg body weight) or saline control. For systemic targeted peptide delivery, mice were treated by tail vein with 200 μg of FITC-CNGRC, FITC-GGGGG, E7 (aa42-63), or CNGRC-E7 peptide, together with intraperitoneal cisplatin (5 mg/kg) or saline control. Mice were monitored for evidence of tumor growth by visual inspection and palpation twice each week. To assess tumor burden in the lung hematogenous spread model, C57BL/6 mice were each inoculated subcutaneously with 10^5 TC-1 cells and treated as described above. Mice were then each inoculated intravenously with 10^5 TC-1 cells on day 9. The number of pulmonary tumor nodules was counted on day 30. For *in vivo* experiments with other pharmacologic agents, we used the following doses per injection of each type of chemotherapy: carboplatin (50 mg/kg), doxorubicin (10 mg/kg), cyclophosphamide (20 mg/kg).

Surface tetramer, intracellular cytokine staining, and flow cytometry

C57BL/6 mice were administered with cisplatin (5 mg/kg) or saline control in conjunction with 20 μg of E7 peptide (aa43-62), 50 μg of TA-CIN, 20 μg of CNGRC-E7 peptide, 20 μg of short Ova peptide (aa257-264), 20 μg of long Ova peptide (aa241-270), 50 μg of Ova protein, or saline control. Mice were boosted twice at the same dose and regimen at 3-day intervals. For tetramer staining, blood and tumor tissue was harvested 1 week after the last peptide or protein injection. Phycoerythrin (PE)-labeled H-$2D^b$ tetramers containing HPV-16 E7 49-57 peptide (RAHYNIVTF) (Beckman Coulter) were used for the analysis of E7-specific $CD8^+$ T cells by flow cytometry (16). For intracellular cytokine staining, splenocytes were harvested 1 week after the last peptide or protein injection. Before intracellular cytokine staining, 6×10^5 pooled splenocytes from each vaccination group were incubated with 1 μg/ml E7 peptide (aa49-57), AH1 peptide (SPSYVYHQF), or Ova peptide

(SIINFEKL), together with GolgiPlug (1000×) (BD Biosciences) for 16 hours. Cells were then harvested and mixed with monoclonal antibodies against CD8 and IFN-γ as we previously described (17). Samples were acquired on a FACSCalibur device using CellQuest Pro software (BD Biosciences). All analysis was carried out on gated lymphocyte populations.

In vivo antibody depletion experiments

C57BL/6 mice (5 per group) were inoculated subcutaneously with 10^5 TC-1 cells per animal and treated with cisplatin (5 mg/kg) and E7 peptide (20 μg) according to the regimen described above. Depletion was initiated 1 day prior to injection of cisplatin and peptide and ended on day 30 after tumor challenge. The following antibody clones were used: CD4 (GK1.5), CD8 (2.43), NK1.1 (PK136). IgG was used as an isotype control.

Analysis of tumor-infiltrating populations

To detect tumor-infiltrating $CD11c^+$ DCs, C57BL/6 mice (3 per group) were inoculated subcutaneously with 10^5 TC-1 cells per animal. On day 5, mice were treated intraperitoneally with cisplatin (5 mg/kg) or saline control twice at 3-day intervals. 1 day after the last injection, tumor tissue was excised from mice, mechanically disrupted into fragments in PBS, washed twice, and digested with 500 U/ml dispase (Godo Shusei) at 37°C for 20 minutes. Tissue fragments were resuspended in 5 ml of PBS and mixed extensively with a Pasteur pipette to obtain single cells. The cells were then passed through a stainless wire sieve (100 mesh) and washed twice with PBS. Sedimented cells were resuspended in PBS and stained with PE-labeled anti-CD11c monoclonal antibody (BD Pharmingen). To detect migration of $CD11c^+$ DCs into lymph nodes, TC-1 tumor-bearing mice were treated with or without cisplatin as described above and administered i.t. with 20 μg of FITC-labeled E7 peptide, with or without 100 nM (4S)-(3-[(3R,S)-3-cyclohexyl-3-hydroxypropyl]-2,5-dioxo)-4-imidazolidineheptanoic acid (BW245C), a migration inhibitor. After 48 hours, draining lymph nodes were harvested and homogenized in RPMI-10 using nylon mesh bags. Erythrocytes were lysed using ammonium chloride, and the remaining cells were washed twice with RPMI-10. Cells were stained with PE-labeled anti-CD11c antibody and allophycocyanin-labeled anti-CD40, -CD80, or -CD86 antibody (BD Pharmingen). To detect tumor-infiltrating T cells, C57BL/6 (3 per group) were inoculated with tumor and treated with cisplatin and/or i.t. E7 peptide as described above. On day 7, tumor tissue was excised and processed as described above. Tumor-infiltrating T cells were stained with FITC-labeled anti-CD8 and PE-labeled E7 tetramer and analyzed by flow cytometry.

T cell activation experiments

C57BL/6 mice (3 per group) were inoculated subcutaneously with 10^5 TC-1 cells per animal. On day 5, mice were treated with cisplatin and/or i.t. E7 peptide (40 μg), with or without 100 nM BW245C. After 48 hours, draining or non-draining lymph nodes were harvested and single cells were prepared as described above. $CD11c^+$ cells were isolated with magnetic beads (Miltenyi Biotec). 2×10^5 $CD11c^+$ DCs were incubated with E7-specific $CD8^+$ T cells overnight at a 1:1 ratio. The frequency of IFN-γ-secreting E7-specific $CD8^+$ T cells was determined by flow cytometry.

ELISA

C57BL/6 mice (5 per group) were inoculated subcutaneously with 10^5 TC-1 cells per animal. On day 5, mice were treated with cisplatin and/or i.t. E7 peptide as described above. On day 7, 10, and 14 after tumor challenge, tumor tissue was excised and processed into single cells as described above. Cells were lysed using Protein Extraction Solution RIPA

(Pierce), and protein concentration was measured by Coomassie Plus protein assay (Pierce). ELISA was performed to quantify levels of Mcp-1 and IFN-β according to the manufacturer's protocol (R&D Systems). All cytokine amounts were normalized to total protein concentration.

Statistical analysis

The data presented in this study are representative of 3 independent experiments, and are expressed as mean ± SD. The number of samples in each group for any given experiment was greater than 3. Results for flow cytometry analysis and tumor treatment experiments were evaluated by one-way analysis of variance (ANOVA) and the Tukey-Kramer test. Individual data points were compared using Student's t-test. The event-time distributions for different mice were compared using the Kaplan-Meier method and the log-rank test. All p values < 0.05 were considered significant.

Results

Chemotherapy with high antigen exposure efficiently controls tumor growth

We first assessed the influence of antigen exposure in the tumor microenvironment on the tumor-specific immune response after chemotherapy. We inoculated C57BL/6 mice with TC-1 tumor cells, which contain the E7 oncogene from human papillomavirus (HPV) type-16(15), and then treated the mice with various combinations of the platinum-based chemotherapy cisplatin, administered into the peritoneal cavity, together with long E7 peptide (aa 42-63) containing H2-D^b-restricted E7 epitope (aa 49-57) administered either directly into the tumor or into subcutaneous (s.c.) tissue (Figure 1A). Bitherapy with cisplatin and intratumor (i.t.) E7 peptide virtually cured TC-1-bearing mice, while monotherapy with either of these reagents led to rapid tumor progression and death (Figure 1, B-D). Cisplatin therapy with s.c. E7 injection failed to control tumor growth (Figure 1, B-D), indicating that priming of the tumor-specific immune response after chemotherapy occurred only with peptide delivery into the tumor microenvironment. While the group of tumor-bearing mice treated with i.t. antigenic peptide following cisplatin remained tumor-free 26 days after tumor challenge, eventually 70% of the tumor-bearing mice in this treatment group develop tumors again 70 days after tumor challenge as shown in Figure 1D. Furthermore, cisplatin and i.t. E7 bitherapy almost completely protected mice from development of pulmonary tumor nodules in a hematogenous spread model, while monotherapy had only a mild protective effect (Figure 1E). Similar results were observed with DNA intercalating agents other than cisplatin (Figure 1F). We conclude that chemotherapy converts the tumor into a microenvironment capable of instigating and sustaining both a productive local and systemic tumor-specific immune response after adjuvant-free peptide vaccination.

Tumor control by chemotherapy and high antigen exposure is mediated through $CD8^+$ cytotoxic T lymphocytes

To characterize this tumor-specific immune response, we depleted $CD4^+$ or $CD8^+$ T cells or NK cells in TC-1-bearing mice with monoclonal antibodies and then treated the mice with cisplatin and i.t. E7 bitherapy. While elimination of $CD4^+$ T cells and NK cells had no effect on tumor growth (data not shown), depletion of $CD8^+$ T cells abolished tumor control by the combined regimen (Figure 2A). There were a large number of E7-specific $CD8^+$ T cells in the tumors of TC-1-bearing mice treated with this regimen (nearly 40% of total $CD8^+$ T cells); by contrast, E7-specific $CD8^+$ T cells were barely detectable among groups of tumor-bearing mice treated either with monotherapy (with cisplatin or i.t. E7) or with cisplatin and s.c. E7 bitherapy (Figure 2B). Similar results were observed in the blood (Figure 2C) and in the spleen (Figure 2D), as well as for different types of chemotherapy (Figure 2E). Thus, we

conclude that the local and systemic anti-tumor effect elicited by chemotherapy, in the context of high antigen density within the tumor, is mediated by $CD8^+$ CTLs.

To extend the translational value of this methodology, we similarly treated TC-1-bearing mice with cisplatin together with i.t. injection of a clinical-grade recombinant E6, E7, and L2 fusion protein (TA-CIN). Cisplatin and i.t. TA-CIN bitherapy elicited a robust E7-specific CTL-mediated immune response and led to tumor eradication and complete long-term survival (Supplemental Figure 1, A-C). Unlike peptide-based vaccination, which has limited potential due to MHC restriction, protein-based vaccination can be applied to individuals with different MHC genetic backgrounds. Furthermore, comparable results were observed in a distinct antigen system, ovalbumin, with either i.t. peptide or protein injection (Supplemental Figure 1, D and E). These data suggest that non-tumor associated antigens can also elicit a potent antigen-specific T cell immune response resulting in an appreciable therapeutic antitumor effect

Chemotherapy induces activation and migration of antigen-loaded dendritic cells into tumor-draining lymph nodes

We next examined the mechanisms by which chemotherapy facilitates development of an adaptive immune response within the tumor microenvironment after adjuvant-free peptide vaccination. We found that following delivery of cisplatin, there was a 10-fold accumulation of $CD11c^+$ DCs in tumor tissue (to 30% of total cells in the tumor) (Figure 3A). To trace the destination and phenotype of these DCs, we co-administered cisplatin and FITC-labeled long E7 peptide (aa 42-63) into the tumor. We then isolated the tumor-draining lymph nodes and assessed the frequency of $FITC^+$ DCs. The amount of $FITC^+$ DCs was amplified over 10-fold in lymph nodes from mice administered with cisplatin compared to isotonic saline control, and co-delivery of the prostaglandin analog BW245C, which inhibits migration of DCs, abrogated this effect (Figure 3B). Furthermore, $FITC^+$ DCs had higher mean expression of the co-stimulatory molecules CD40, CD80, and CD86 relative to $FITC^-$ DCs (Figure 3C). We found that DCs isolated from mice treated with i.t. E7 in conjunction with cisplatin activated E7-specific CTLs over 15 times more strongly than DCs from mice administered with i.t. E7 alone, but this effect was lost with co-injection of BW245C (Figure 3D). In addition, E7-specific CTLs failed to become activated when mixed with DCs from lymph nodes of mice treated with cisplatin alone, demonstrating that the density of E7 antigen within the endogenous TC-1 tumor microenvironment is insufficient for development of a tumor-specific adaptive immune response (Figure 3D). These data indicate that chemotherapy enriches DCs in the tumor microenvironment; these DCs have the capacity to uptake tumor antigen, whereupon they mature, travel to the draining lymph nodes, and prime tumor-specific CTLs.

The type-I interferon and Toll-like receptor 4 (TLR4) signaling axes are required for the tumor-specific immune response elicited by chemotherapy

We next explored the molecular signaling axes underlying the priming of an adaptive immune response in the tumor microenvironment after chemotherapy. We found that for over 2 weeks after cisplatin injection, there was a greater than 10-fold rise in the tumor in the concentration of the chemokine Ccl2 (Mcp-1), which has a major function in recruiting DCs to inflammatory sites (Figure 4A). Furthermore, the levels of IFN-β in the tumor were also persistently elevated over 10-fold after cisplatin injection (Figure 4B), suggesting a role for the type-I interferon pathway in the immune-modulating effect of chemotherapy. In support of this, DCs from transgenic mice deficient in IFN-α receptor (IFNAR) failed to uptake FITC-labeled E7 peptide and move into draining lymph nodes after cisplatin and i.t. E7 injection (Figure 4C). $IFNAR^{-/-}$ mice also mounted a systemic immune response 5 times weaker than wild type littermates, after cisplatin and i.t. E7 bitherapy (Figure 4D), which

correlated with lack of tumor control (Figure 4E) and reduced survival (Figure 4F). We conducted parallel experiments in TLR4-deficient mice and found the effectiveness of cisplatin and i.t. E7 bitherapy to also depend on the TLR4 pathway (Figure 5, A-D), as has been previously suggested(8). Tumor cells are likely a direct source for triggering this pathway in DCs since TC-1 cells treated with cisplatin release a large amount of the TLR4 ligand HMGB1 (Supplemental Figure 2). We conclude that the type-I interferon and TLR4 axes mediate the immune-modulating effect of chemotherapy in the tumor microenvironment. It will be important to further elucidate the precise relationship between the type-I interferon and TLR4 axes as it relates to this effect.

Chemotherapy enables vaccine adjuvant-free priming of a tumor-specific immune response against self tumor antigen

To extend our study outside the realm of viral-associated cancer—which presents a straightforward target for immune control due to the expression of foreign tumor antigen—we adopted the CT26 model of colon cancer, which was derived by chemical carcinogenesis(18). The epitope AH1-A5 of gp70 has previously been identified as a self-antigen in the CT26 model capable of expanding tumor-reactive CTLs(19). Thus, we treated CT26-bearing mice with cisplatin together with i.t. AH1-A5 peptide (Figure 6A). This combined regimen led to sustained, stable control of disease (Figure 6B), prolonged survival of mice (Figure 6C), and a higher frequency of AH1-A5-specific CTLs (Figure 6D) compared to either monotherapy (with cisplatin or i.t. AH1-A5) or bitherapy with cisplatin and s.c. AH1-A5. We conclude that chemotherapy supports the priming of an adaptive immune response within the tumor against foreign as well as self tumor antigen. Thus, the immune-based therapy described here represents a universal approach, which may be effective against a wide spectrum of cancer types.

Chemotherapy together with targeted systemic delivery of antigen to the tumor is an effective approach to control cancer

Since down-regulation or loss of tumor antigen is a prevalent—and sometimes predominant—mode of tumor immune escape(20), the delivery of exogenous antigen into the tumor microenvironment may be a requirement in the clinical setting. However, i.t. injection is often impractical as a means of antigen delivery, particularly in the context of disseminated cancer or a tumor embedded deeply within solid tissue. To overcome this hurdle, we employed the CD13-binding peptide CNGRC to target antigen to tumor tissue after systemic injection. CD13 is an aminopeptidase abundantly present on the surface of tumor endothelial cells and thus represents a suitable target for antigen delivery to the tumor(21, 22). After intravenous (i.v.) injection of FITC-labeled CNGRC peptide into TC-1-bearing mice, over 5% of cells harvested from tumor tissue were $FITC^+$ (compared to only 0.1% of cells from tumor of mice administered with FITC-labeled GGGGG control peptide) (Figure 7A); of these $FITC^+$ cells, over 15% were $CD11c^+$ DCs (Figure 7B). Furthermore, tumor-infiltrating $CD11c^+$ DCs isolated from mice administered by i.v. route with CNGRC-conjugated E7 peptide had 5 times greater capacity to activate E7-specific CTLs compared to those from mice administered with unconjugated E7 peptide (Figure 7C). Combined delivery of cisplatin and i.v. CNGRC-E7 also led to strong inhibition of tumor growth and control of disease in TC-1-bearing mice (Figure 7, D-F). Notably, mice administered CNGRC-E7 alone had identical tumor growth kinetics as those administered saline control (Figure 7, D-F), indicating that high antigen exposure in the tumor is by itself incapable of producing a potent tumor-specific immune response. Indeed, mice administered with cisplatin together with CNGRC-E7 had much a greater systemic E7-specific CTL-mediated immune response than mice administered with either agent alone (Figure 7, G and H). Thus, we have provided a proof-of-principle demonstration that the therapy developed here can be readily and conveniently applied to the clinical management of a wide variety of human cancer types.

In summary, our study reveals for the first time that the tumor microenvironment is converted by chemotherapy into a site permissive for vaccination to elicit a local and systemic immune response without the need for additional adjuvant. This immune response is driven by the accumulation of DCs in the tumor, followed by their maturation, migration to lymph nodes, and priming of tumor-specific $CD8^+$ CTLs in a type I-interferon-dependent manner. Our data further indicate that antigen density within the tumor is an important determinant of the outcome of immune surveillance following chemotherapy. These findings have significant clinical implications and introduce a new direction for the development of immune-based therapy for cancer.

Discussion

In this study, we have shown that a broad range of pharmacologic agents for cancer therapy fundamentally alters the tumor microenvironment into a site that permits a productive tumor-specific local and systemic immune response. These results demonstrate that while the tumor might predominately exist in an immune-suppressive state, this state is highly dynamic and can be reversed by pharmacologic intervention. Thus, our data provide impetus for the development and clinical translation of novel immune-based strategies for cancer therapy.

We found that antigen delivery into the tumor in the context of chemotherapy was sufficient to generate a strong antigen-specific $CD8^+$ CTL immune response, which led to effective and persistent control of local and disseminated disease. Notably, our approach applies broadly regardless of the type of antigen (peptide or protein) or the class of chemotherapy. Furthermore, the approach can be extended to antigens not directly associated with the tumor. For example,we observed that i.t. injection with foreign peptide (Ova) led to the generation of Ova-specific CD8+ T cells as well as therapeutic antitumor effects against non-Ova expressing tumors (Supplemental Figure 1).

Several potential mechanisms may account for the observed antitumor therapeutic effects generated by the i.t. injection of Ova. For example, the uptake of Ova by tumor stromal cells, such as CD11b+ myeloid derived cells, may lead to the processing and presentation of Ova peptide through the class I MHC pathway, rendering CD11b+ myeloid cells susceptible to Ova-specific CD8+ T cell-mediated killing. Zhang, et al previously observed that treatment of tumors with a chemotherapeutic drug could lead to the loading of CD11b+ tumor stromal cells with tumor-specific peptide presented by MHC class I molecules (23). Thus, our study is consistent with Zhang's study in that the CD11b+ tumor stromal cells are capable of processing and presenting the antigenic peptide making them sensitized for T cell-mediated killing. Additionally, the antitumor effect generated by our approach may lead to the release of tumor antigen, such as E7 in TC-1 tumors, resulting in enhanced cross-priming of CD8+ T cells reactive against intrinsic E7. Thus, the antitumor effect observed following the i.t. injection of antigen, such as Ova, may be accounted for by different mechanisms.

In addition to being effective using a variety of antigens, our approach does not require administration of exogenous adjuvants beyond chemotherapy. The vast majority of vaccination regimens for cancer or infectious disease rely on adjuvants in order to create a potent immune response. However, very few adjuvants have been approved for clinical use, and the administration of adjuvants carries intrinsic risks of substantial side effects. Thus, our study has important translational value. From a scientific point of view, the ability of chemotherapy to elicit an adaptive immune response within the tumor in the absence of vaccine adjuvants indicates that the tumor microenvironment is an ideal site for the priming of CTLs. Notably, delivery of antigen into subcutaneous tissue—the most common

vaccination site—without adjuvants did not elicit a detectable immune response. This discovery challenges the prevailing notion of the tumor as an inherently immune-suppressive site and underscores the dynamic nature of interactions between the tumor and the immune system. We posit a model in which the tumor is at equilibrium in an immune-suppressive state imposed by an inhibitory cytokine milieu, an extensive checkpoint network, and an abundance of regulatory immune cells. This immune-suppressive state is opposed by a variety of components, including pro-inflammatory factors, stimulatory immune cells, and effector CTLs. Our study reveals that chemotherapy shifts this balance of forces in favor of an immune-supportive state within the tumor.

In the current study, we have observed the accumulation of CD11c+ DCs in the tumor after treatment with cisplatin, which led to enhanced activation of antigen-specific CD8+ T cells subsequent to i.t. injection of antigen. We have explored several factors that may contribute to the observed phenomenon. We observed that MCP-1 (CCL2) was upregulated following chemotherapy (Figure 4A). MCP-1 was previously shown to be closely related to the migration of DCs (24, 25). Thus, the upregulation of MCP-1 may account for the accumulation of CD11c+ DCs in tumor loci, although we cannot exclude the contribution of other molecules to this process.

In the current study, we focused on the TLR4 and type 1 interferon activation pathways for the generation of antigen-specific CD8+ T cells. It has previously been shown that the anticancer immune response induced by chemotherapy is dependent on the contribution of TLR4 and involves HMGB-1 action on TLR4 (8). We have observed that tumor cell treatment with cisplatin can lead to the release of HMGB1 (see Supplemental Figure 2). The release of HMGB1 is likely important for the activation of the TLR4 pathway. Previously, it has been shown that the type 1 interferon pathway is involved in the maturation and migration of dendritic cells and T cell priming (26). Consequently, we focused on the type 1 interferon pathway. We have observed that the activation of both the type 1 interferon and TLR4 pathways is important for the generation of antigen-specific CD8+ T cells.

By examining the influence of Mcp-1 along with the TLR4 and type 1 interferon pathways, we have identified a potential mechanism through which the immune-supportive state is established in the tumor. In particular, chemotherapy induces the infiltration of DCs into the tumor. Upon encounter with antigen, these DCs undergo activation and migration to draining lymph nodes where they stimulate tumor-specific CTLs. The infiltration of DCs into the tumor is most likely mediated by the chemokine Mcp-1, as we observed elevated levels of this chemokine in the tumor following chemotherapy. Furthermore, the maturation of DCs and their migration to lymph nodes is dependent on the type-I interferon pathway, as (1) IFN-β levels were increased in the tumor after chemotherapy and (2) IFNAR-deficient mice exhibit defective migration of antigen-loaded DCs into tumor-draining lymph nodes, as well as severely compromised immune response and anti-tumor effects following vaccination. The release of type-I interferon in DCs is most likely triggered through the TLR4 pathway, as the immune-stimulatory effects of chemotherapy are abolished in TLR4-deficient mice. Notably, tumor cells treated with chemotherapy release high levels of HMGB1, a ligand for TLR4. Taken together, one possible scenario underlying the immune-stimulatory effects of chemotherapy on the tumor microenvironment is: (1) chemotherapy causes tumor cells to release HMGB1, (2) HMGB1 binds to TLR4 on resident DCs and causes them to secrete Mcp-1 and type-I interferon, (3) Mcp-1 attracts a large number of DCs into the tumor, while type-I interferon induces their maturation and migration into draining lymph nodes, (4) antigen-loaded DCs stimulate cognate CTLs to attack the tumor. Apparently, there are other potential pathways and/or sequences that may contribute to the observed phenomena in our study. Additionally, we observed that chemotherapy also reduces the number of systemic myeloid-derived suppressor cells in tumor-bearing mice

(Supplemental Figure 3), and shifts the macrophage population in the tumor towards a stimulatory M1 phenotype (Supplemental Figure 4).

This model also explains our observation that antigen density within the tumor is an important determinant of the immune response and clinical outcome. Consistent with this idea, we found that within the lymph nodes, DCs loaded with tumor antigen had higher activation status than DCs without antigen. Thus, we conclude that a precondition for a successful outcome for any immune-based therapy following chemotherapy is sufficient antigen exposure within the tumor. With this concept, we have developed a new approach to immune-based therapy based on targeted antigen delivery into the tumor in conjunction with chemotherapy (see Figure 7). This approach is especially powerful because it can be used conveniently to control antigen density within the tumor. We envision that such a technology could be widely implemented with either peptide or protein antigen. Furthermore, this technology could in principle be readily applied to any tumor type with defined antigen. In a case in which the tumor does not possess any such defined antigen, we propose that a foreign antigen—for example, a viral antigen that many individuals have pre-existing memory CTLs against—may instead be targeted to the tumor. We therefore believe that this approach may warrant future clinical translation.

Supplementary Material

Refer to Web version on PubMed Central for supplementary material.

Acknowledgments

We thank Ms. Jayne Knoff for preparation of this manuscript.

Grant Support

This work was funded by the National Institutes of Health Cervical Cancer SPORE and Head and Neck Cancer SPORE (P50 CA098252 and P50 CA96784-06) and RO-1 grant (CA114425-01).

References

1. Galluzzi L, Senovilla L, Zitvogel L, Kroemer G. The secret ally: immunostimulation by anticancer. Nature reviews Drug discovery. 2012; 11:215–33.
2. Zitvogel L, Apetoh L, Ghiringhelli F, Kroemer G. Immunological aspects of cancer chemotherapy. Nature reviews Immunology. 2008; 8:59–73.
3. Ghiringhelli F, Apetoh L, Tesniere A, Aymeric L, Ma Y, Ortiz C, et al. Activation of the NLRP3 inflammasome in dendritic cells induces IL-1beta-dependent adaptive immunity against tumors. Nature medicine. 2009; 15:1170–8.
4. Obeid M, Tesniere A, Ghiringhelli F, Fimia GM, Apetoh L, Perfettini JL, et al. Calreticulin exposure dictates the immunogenicity of cancer cell death. Nature medicine. 2007; 13:54–61.
5. Michaud M, Martins I, Sukkurwala AQ, Adjemian S, Ma Y, Pellegatti P, et al. Autophagy-dependent anticancer immune responses induced by chemotherapeutic agents in mice. Science. 2011; 334:1573–7. [PubMed: 22174255]
6. Martins I, Kepp O, Schlemmer F, Adjemian S, Tailler M, Shen S, et al. Restoration of the immunogenicity of cisplatin-induced cancer cell death by endoplasmic reticulum stress. Oncogene. 2011; 30:1147–58. [PubMed: 21151176]
7. Casares N, Pequignot MO, Tesniere A, Ghiringhelli F, Roux S, Chaput N, et al. Caspase-dependent immunogenicity of doxorubicin-induced tumor cell death. The Journal of experimental medicine. 2005; 202:1691–701. [PubMed: 16365148]
8. Apetoh L, Ghiringhelli F, Tesniere A, Obeid M, Ortiz C, Criollo A, et al. Toll-like receptor 4-dependent contribution of the immune system to anticancer chemotherapy and radiotherapy. Nature medicine. 2007; 13:1050–9.

9. Lake RA, Robinson BW. Immunotherapy and chemotherapy--a practical partnership. Nature reviews Cancer. 2005; 5:397–405.
10. Yang Y, Liu C, Peng W, Lizee G, Overwijk WW, Liu Y, et al. Antitumor T-cell responses contribute to the effects of dasatinib on c-KIT mutant murine mastocytoma and are potentiated by anti-OX40. Blood. 2012; 120:4533–43. [PubMed: 22936666]
11. Nakasone ES, Askautrud HA, Kees T, Park JH, Plaks V, Ewald AJ, et al. Imaging tumor-stroma interactions during chemotherapy reveals contributions of the microenvironment to resistance. Cancer cell. 2012; 21:488–503. [PubMed: 22516258]
12. Kepp O, Galluzzi L, Martins I, Schlemmer F, Adjemian S, Michaud M, et al. Molecular determinants of immunogenic cell death elicited by anticancer chemotherapy. Cancer metastasis reviews. 2011; 30:61–9. [PubMed: 21249425]
13. Ko JS, Zea AH, Rini BI, Ireland JL, Elson P, Cohen P, et al. Sunitinib mediates reversal of myeloid-derived suppressor cell accumulation in renal cell carcinoma patients. Clinical cancer research : an official journal of the American Association for Cancer Research. 2009; 15:2148–57. [PubMed: 19276286]
14. Rabinovich GA, Gabrilovich D, Sotomayor EM. Immunosuppressive strategies that are mediated by tumor cells. Annual review of immunology. 2007; 25:267–96.
15. Lin KY, Guarnieri FG, Staveley-O'Carroll KF, Levitsky HI, August JT, Pardoll DM, et al. Treatment of established tumors with a novel vaccine that enhances major histocompatibility class II presentation of tumor antigen. Cancer research. 1996; 56:21–6. [PubMed: 8548765]
16. Clay TM, Hobeika AC, Mosca PJ, Lyerly HK, Morse MA. Assays for monitoring cellular immune responses to active immunotherapy of cancer. Clinical cancer research : an official journal of the American Association for Cancer Research. 2001; 7:1127–35. [PubMed: 11350875]
17. Cheng WF, Hung CF, Lin KY, Ling M, Juang J, He L, et al. CD8+ T cells, NK cells and IFN-gamma are important for control of tumor with downregulated MHC class I expression by DNA vaccination. Gene therapy. 2003; 10:1311–20. [PubMed: 12883527]
18. Daayana S, Elkord E, Winters U, Pawlita M, Roden R, Stern PL, et al. Phase II trial of imiquimod and HPV therapeutic vaccination in patients with vulval intraepithelial neoplasia. British journal of cancer. 2010; 102:1129–36. [PubMed: 20234368]
19. Fiander AN, Tristram AJ, Davidson EJ, Tomlinson AE, Man S, Baldwin PJ, et al. Prime-boost vaccination strategy in women with high-grade, noncervical anogenital intraepithelial neoplasia: clinical results from a multicenter phase II trial. International journal of gynecological cancer : official journal of the International Gynecological Cancer Society. 2006; 16:1075–81. [PubMed: 16803488]
20. Smyth LJ, Van Poelgeest MI, Davidson EJ, Kwappenberg KM, Burt D, Sehr P, et al. Immunological responses in women with human papillomavirus type 16 (HPV-16)-associated anogenital intraepithelial neoplasia induced by heterologous prime-boost HPV-16 oncogene vaccination. Clinical cancer research : an official journal of the American Association for Cancer Research. 2004; 10:2954–61. [PubMed: 15131030]
21. Belnap LP, Cleveland PH, Colmerauer ME, Barone RM, Pilch YH. Immunogenicity of chemically induced murine colon cancers. Cancer research. 1979; 39:1174–9. [PubMed: 84709]
22. Hibbitts S. TA-CIN, a vaccine incorporating a recombinant HPV fusion protein (HPV16 L2E6E7) for the potential treatment of HPV16-associated genital diseases. Current opinion in molecular therapeutics. 2010; 12:598–606. [PubMed: 20886392]
23. Zhang B, Bowerman NA, Salama JK, Schmidt H, Spiotto MT, Schietinger A, et al. Induced sensitization of tumor stroma leads to eradication of established cancer by T cells. The Journal of experimental medicine. 2007; 204:49–55. [PubMed: 17210731]
24. Nakamura K, Williams IR, Kupper TS. Keratinocyte-derived monocyte chemoattractant protein 1 (MCP-1): analysis in a transgenic model demonstrates MCP-1 can recruit dendritic and Langerhans cells to skin. The Journal of investigative dermatology. 1995; 105:635–43. [PubMed: 7594634]
25. Vanbervliet B, Homey B, Durand I, Massacrier C, Ait-Yahia S, de Bouteiller O, et al. Sequential involvement of CCR2 and CCR6 ligands for immature dendritic cell recruitment: possible role at

inflamed epithelial surfaces. European journal of immunology. 2002; 32:231–42. [PubMed: 11782014]

26. Nagai T, Devergne O, Mueller TF, Perkins DL, van Seventer JM, van Seventer GA. Timing of IFN-beta exposure during human dendritic cell maturation and naive Th cell stimulation has contrasting effects on Th1 subset generation: a role for IFN-beta-mediated regulation of IL-12 family cytokines and IL-18 in naive Th cell differentiation. J Immunol. 2003; 171:5233–43. [PubMed: 14607924]

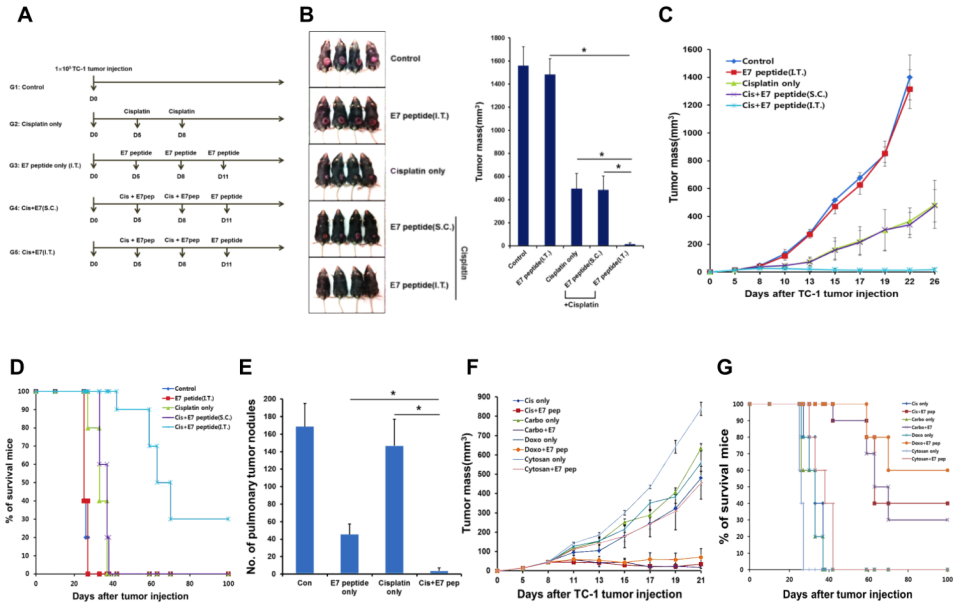

Figure 1. Disease outcome in tumor-bearing mice treated with chemotherapy and intratumor peptide injection

C57BL/6 mice were inoculated subcutaneously with TC-1 tumor cells and treated with various combinations of chemotherapy and E7 peptide, as indicated. Parameters of disease outcome were scored over time. (A) Schematic diagram of therapy regimen. (B) Tumor size in mice at a static time point. Left: Digital photograph of tumor size on day 25 after tumor challenge. Right: Bar graph quantification of tumor size (mean ± SD). (C) Scatter plot of tumor growth kinetics. (D) Kaplan–Meier survival plot. (E) Tumor-bearing mice treated as illustrated in (A) were inoculated intravenously with TC-1 cells on day 9. The number of pulmonary tumor nodules was counted on day 30 (mean ± SD). (F) Scatter plot of tumor growth kinetics in mice treated with different classes of chemotherapy. **(G) Kaplan–Meier survival plot.**

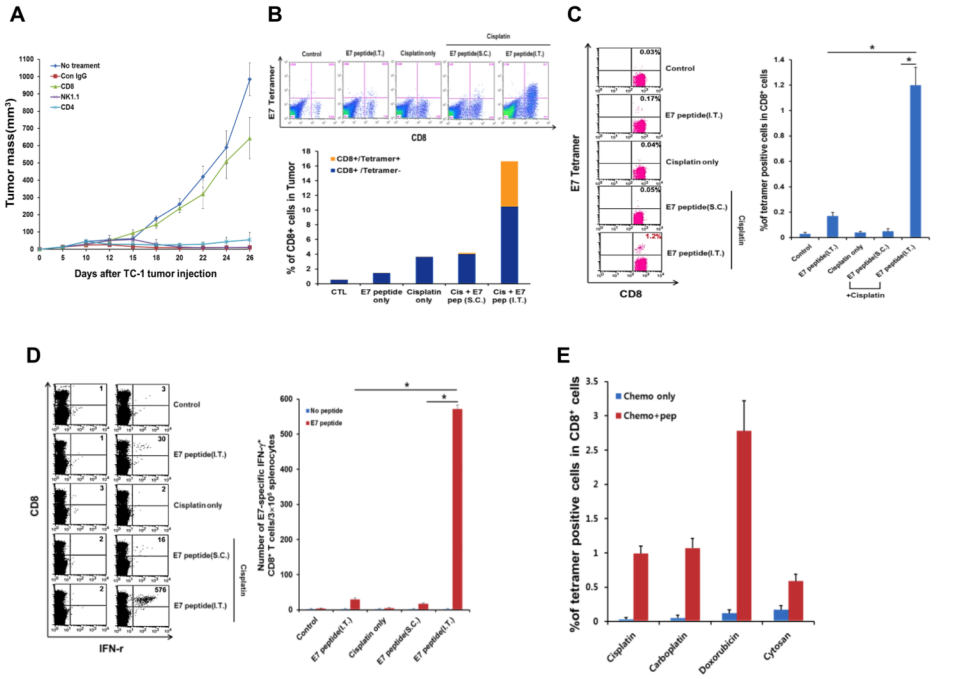

Figure 2. Adaptive immune response in mice treated with chemotherapy and intratumor peptide injection

C57BL/6 mice were inoculated subcutaneously with TC-1 tumor cells and treated with various combinations of chemotherapy and E7 peptide as indicated. Immune cell subsets were analyzed one week after the last antigen delivery (A) Scatter plot of TC-1 growth kinetics in mice treated with cisplatin and i.t. E7 peptide, together with monoclonal antibody against CD8, **NK1.1, CD4, isotype control or no treatment.** Antibody depletion was initiated 1 day prior to therapy and ended on day 30 following tumor challenge. (B and C) Flow cytometry dot plot and bar graph (mean ± SD) depicting the frequency of E7 tetramer-binding $CD8^+$ T cells (top-right quadrant) in the tumor (B) or in the circulation (C). (D) Left: Flow cytometry dot plot depicting the frequency of IFN-γ-secreting $CD8^+$ T cells (top-right quadrant) in the spleen. Right: Bar graph quantification of the data (mean ± SD). (E) Bar graph depicting the frequency of E7 tetramer-binding $CD8^+$ T cells in mice treated with different classes of chemotherapy (mean ± SD).

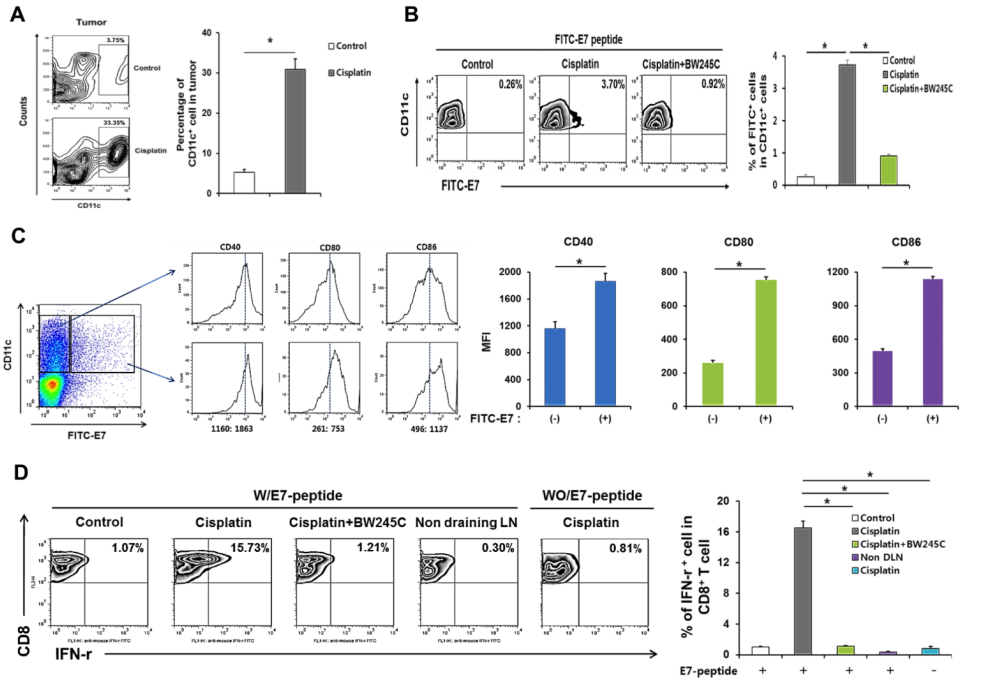

Figure 3. Tumor infiltration, migration to draining lymph nodes, and maturation of CD11c$^+$ dendritic cells in mice treated with chemotherapy and intratumor peptide injection

C57BL/6 mice were inoculated with TC-1 tumor cells and treated with cisplatin and/or i.t. FITC-labeled E7 peptide as indicated. Immune cell subsets were analyzed one week after the last antigen delivery (A) Left: Flow cytometry contour plot depicting the frequency of CD11c$^+$ cells in the tumor with or without cisplatin therapy. Right: Bar graph quantification of the data (mean ± SD). (B) Left: Flow cytometry density plot depicting the frequency of FITC-E7$^+$ CD11c$^+$ DCs in the draining lymph nodes (top-right quadrant). Right: Bar graph quantification of the data (mean ± SD). BW245C was used as an inhibitor of migration. (C) Left: Flow cytometry histogram depicting the expression of activation surface markers (CD40, CD80, and CD86) in CD11c$^+$ DCs with or without FITC-E7 uptake. Right: Bar graph quantification of the data (MFI ± SD). (D) Left: Flow cytometry density plot depicting the production of IFN-γ by CD8$^+$ T cells (top-right quadrant) mixed with CD11c$^+$ cells isolated from tumor-draining lymph nodes of mice treated as indicated. Right: Bar graph quantification of the data (mean ± SD).

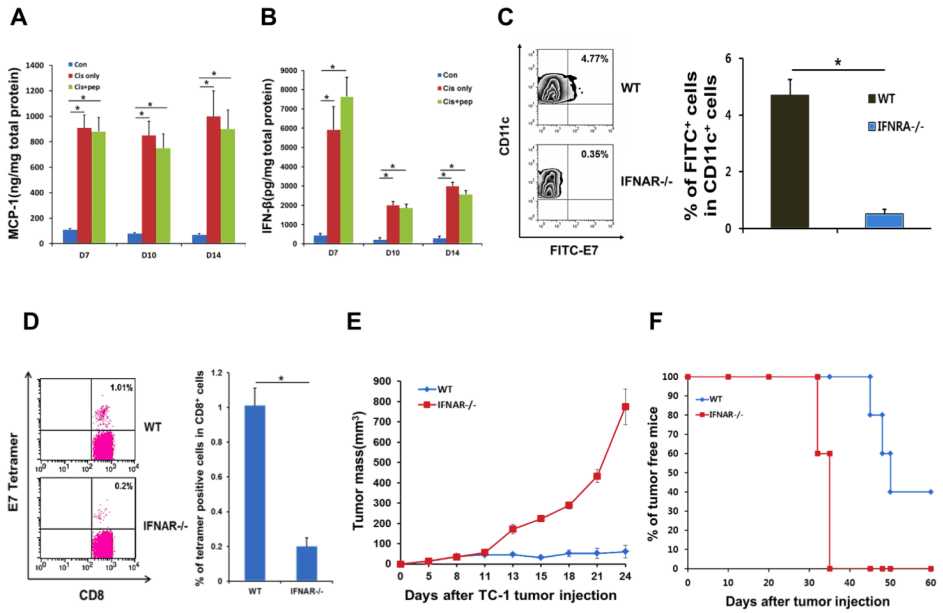

Figure 4. Requirement of the type-I interferon pathway in the immune-modulating effects of chemotherapy

(A and B) TC-1 tumor-bearing C57BL/6 mice were treated with cisplatin, cisplatin and intratumor (i.t.) E7 peptide, or isotonic saline control. Bar graph depicting the concentration of Mcp-1 (A) and IFN-β (B) in excised tumor tissue (mean ± SD). (C-F) IFN-α receptor (IFNAR)-deficient mice or their wild type littermates were inoculated subcutaneously with TC-1 tumor cells and then treated with cisplatin and i.t. E7 peptide bitherapy. Immune cell subsets were analyzed one week after the last antigen delivery. (C) Left: Flow cytometry density plot depicting the frequency of FITC-E7^{+} CD11c^{+} DCs in the draining lymph nodes (top-right quadrant). Right: Bar graph quantification of the data (mean ± SD). (D) Left: Flow cytometry dot plot depicting the frequency of E7 tetramer-binding CD8^{+} T cells (top-right quadrant) in the circulation. Right: Bar graph quantification of the data (mean ± SD). (E) Scatter plot of tumor growth kinetics. (F) Kaplan–Meier survival plot.

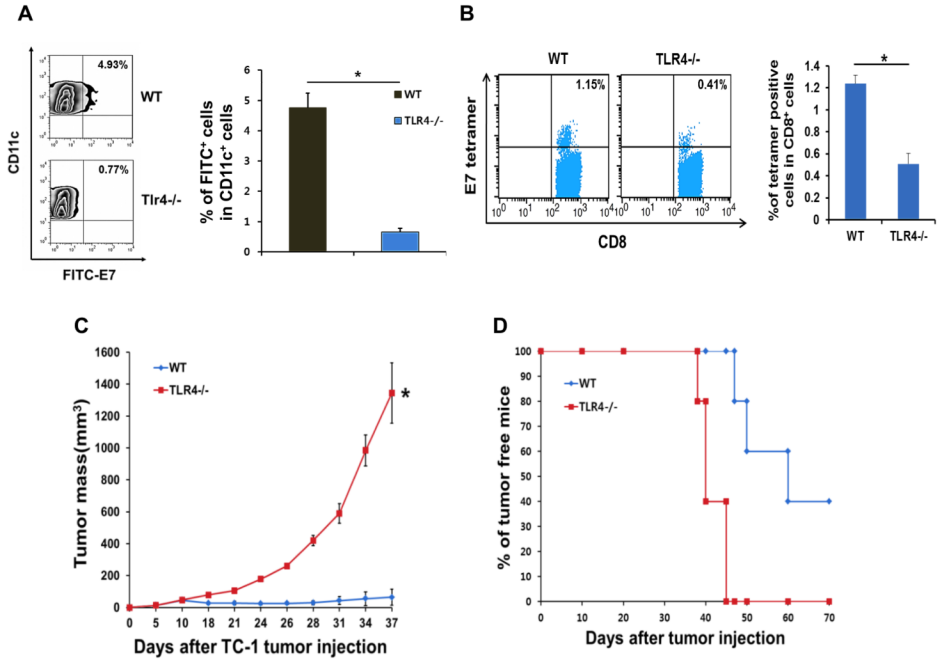

Figure 5. Requirement of the Toll-like receptor 4 (TLR4) pathway in the immune-modulating effects of chemotherapy

(A-D) TLR4-deficient mice or their wild type littermates were inoculated subcutaneously with TC-1 tumor cells and treated with cisplatin and intratumor E7 peptide bitherapy. Immune cell subsets were analyzed one week after the last antigen delivery (A) Left: Flow cytometry density plot depicting the frequency of FITC-E7$^+$ CD11c$^+$ DCs in the draining lymph nodes (top-right quadrant). Right: Bar graph quantification of the data (mean ± SD). (B) Left: Flow cytometry dot plot depicting the frequency of E7 tetramer-binding CD8$^+$ T cells (top-right quadrant) in the circulation. Right: Bar graph quantification of the data (mean ± SD). (C) Scatter plot of tumor growth kinetics. (D) Kaplan–Meier survival plot.

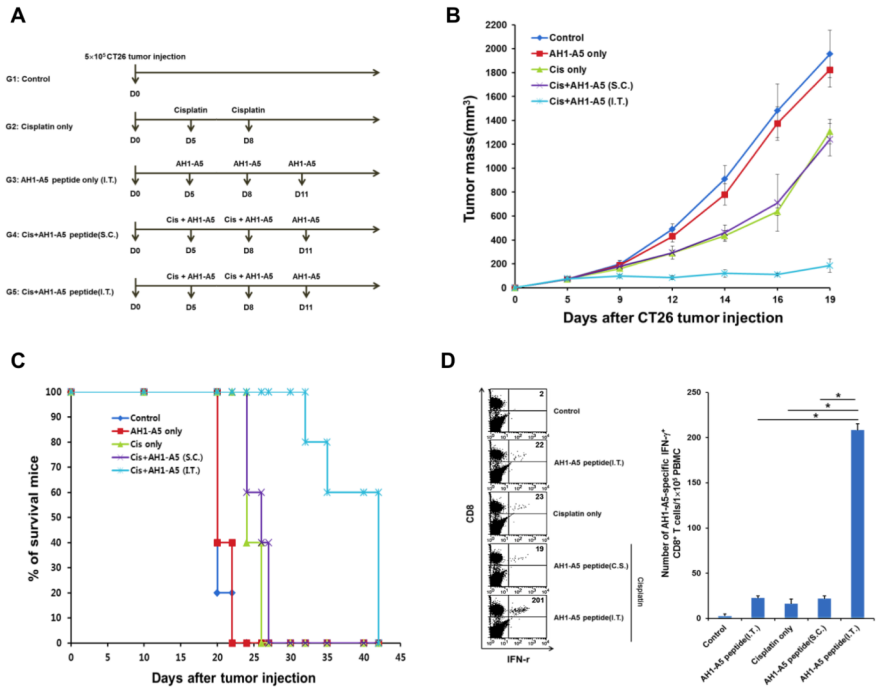

Figure 6. Immune response to a self tumor antigen elicited by chemotherapy and intratumor peptide injection

BALB/c mice were inoculated subcutaneously with CT26 tumor cells and treated with various combinations of cisplatin and the self tumor antigen AH1-A5, as indicated. Immune cell subsets were analyzed one week after the last antigen delivery (A) Schematic diagram of the therapy regimen. (B) Scatter plot of tumor growth kinetics. (C) Kaplan–Meier survival plot. (D) Left: Flow cytometry dot plot depicting the frequency of IFN-γ-secreting $CD8^+$ T cells (top-right quadrant) in the circulation. Right: Bar graph quantification of the data (mean ± SD).

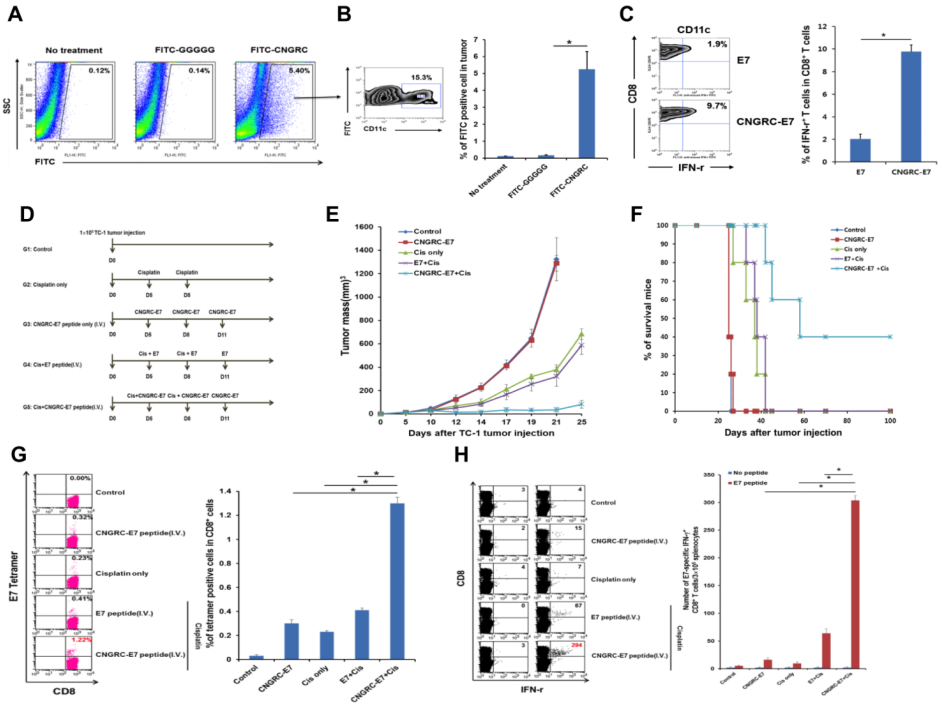

Figure 7. Targeted systemic delivery of antigen to the tumor in conjunction with chemotherapy as a new approach to control cancer

(A and B) C57BL/6 mice were inoculated subcutaneously with TC-1 tumor cells and administered intravenously with FITC-labeled CNGRC peptide or GGGGG control peptide. Immune cell subsets were analyzed one week after the last antigen delivery. (A) Flow cytometry dot plot depicting the total frequency of $FITC^+$ cells in the tumor. (B) Left: Flow cytometry density plot of the frequency of $CD11c^+$ DCs in the tumor that uptook FITC-labeled peptide. Right: Bar graph quantification of the data (mean ± SD). (C) TC-1 bearing mice were administered intravenously with either E7 or CNGRC-E7 peptide. $CD11c^+$ DCs were then isolated from the tumor and mixed with E7-specific $CD8^+$ T cells. Left: Left: Flow cytometry density plot depicting the production of IFN-γ by $CD8^+$ T cells (top-right quadrant). Right: Bar graph quantification of the data (mean ± SD). (D-H) C57BL/6 mice were inoculated subcutaneously with TC-1 cells and treated with various combinations of cisplatin and systemic E7 or CNGRC-E7, as indicated. (D) Schematic diagram of the therapy regimen. (E) Scatter plot of tumor growth kinetics. (F) Kaplan–Meier survival plot. (G) Left: Flow cytometry dot plot depicting the frequency of E7 tetramer-binding $CD8^+$ T cells (top-right quadrant) in the circulation. Right: Bar graph quantification of the data (mean ± SD). (H) Left: Flow cytometry dot plot depicting the frequency of IFN-γ-secreting $CD8^+$ T cells (top-right quadrant) in the spleen. Right: Bar graph quantification of the data (mean ± SD).